MALAYSIAN JOURNAL OF SCIENCE
MJS
ISSN 1394 - 3065

2nd Euro-Asia Conference on CO_2 Capture and Utilization (EACCO2CU2022) Special issue

Malaysian Journal of Science 43 (Special Issue 1): 38-43 (July 2024) https://mjs.um.edu.my

MORINGA OLEIFERA (MO) SEED SHELL BASED ADSORBENT FOR POTENTIAL CO_2 CAPTURE: A CHARACTERIZATION STUDY

Amina Tahreen[1a], Mohammed Saedi Jami[2a*], Fathilah Ali[3a] and Zahangir Alam[4a]

Abstract: This study characterizes activated carbon synthesized from *Moringa oleifera (MO)* seed husk with a greener activating agent, namely sodium carbonate, (Na_2CO_3) compared to traditional activating agent, potassium hydroxide (KOH). Synthesized in a conventional tube furnace with nitrogen supply, the resulting activated carbon after cooling and washing, were characterized for Brunauer-Emmett-Teller (BET), Fourier-Transform Infrared Spectroscopy (FTIR), X-ray Diffraction (XRD) and Scanning Electron Microscope (SEM) analyses and compared with that produced with KOH activation. Although fewer and larger mesoporous activated carbon with smaller BET surface area (18.4659 m^2/g) were formed with Na_2CO_3 activation), compared to that of KOH activation (235.6034 m^2/g), this study highlights the ability and potential of the greener activating agent (Na_2CO_3) to utilize biomass waste and successfully produce activated carbon with minimum environmental hazards. The synthesized adsorbent can be explored for CO_2 capture applications in future studies.

Keywords: Adsorbent synthesis, Moringa oleifera (MO), greener activating agent.

1. INTRODUCTION

The growing concerns regarding greenhouse gas emissions on a global scale has prompted significant research and development efforts towards mitigating the effects through greener approaches. One prominent greenhouse gas is carbon dioxide (CO_2), which is largely generated through the combustion of fossil fuels. To combat the increasing CO_2 levels in the atmosphere, the development of effective and sustainable carbon capture technologies has become vital. Furthermore, as finite natural resources like fossil fuels diminish, and the combustion of coke generates CO_2 emissions, there is a demand for improved approaches to handle and utilize stockpiled coke. Converting biomass waste into activated carbon presents a resolution to address both waste management concerns and the necessity for CO_2 capture (Serafin et al., 2021). Activated carbon, with its exceptional adsorption properties, has emerged as a possible promising material for CO_2 capture (Abuelnoor et al., 2021; Varma, 2019). Its high surface area and pore structure provide ample opportunities for gas molecules, including CO_2, to be adsorbed, thereby, reducing their concentration in the atmosphere.

However, the conventional production methods of activated carbon often involve energy-intensive processes and the use of non-renewable resources, limiting their environmental viability. Hence, in this paper, a sustainable approach towards preparing a green activated carbon is proposed, focusing not only on the activation agent but also on the precursor material. *Moringa oleifera (MO),* a fast-growing tree found in tropical and subtropical regions, produces seeds, the husks of which are typically discarded as biomass waste. The use of *MO* seed husk as a raw material offers several environmental benefits (Yamaguchi et al., 2021). By repurposing this agricultural waste, the pressure on landfills and the need for conventional raw materials such as wood or coal, can be minimized. Additionally, *MO* seed husk (as shown in Figure 1) contains natural cellulose and lignin, which can serve as precursors for the carbonization process, ensuring the formation of a porous structure in the resulting activated carbon (González-García, 2018).

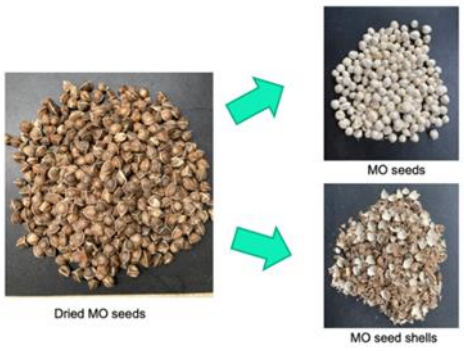

Figure 1. Dried *MO* seeds and separated husk.

However, the current strategies for producing activated carbons involve use of corrosive and hazardous chemical activating agents, typically potassium hydroxide (KOH) (Sevilla et al., 2021) and phosphoric acid (H_3PO_4) (Raji et al., 2023), limiting environmental safety in industrial applications. Hence, this study explores utilizing this sustainable precursor material with sodium carbonate (Na_2CO_3) as the green activation agent, which is a sodium based activating agent in terms of health hazard (Sevilla et al., 2021). The combination of a renewable precursor and an

Authors information:
[a]Department of Chemical Engineering and Sustainability, International Islamic University Malaysia, Kuala Lumpur, Malaysia. E-mail: aminatahreen@gmail.com[1], saedi@iium.edu.my[2], fathilah@iium.edu.my[3], zahangir@iium.edu.my[4]

*Corresponding Author: saedi@iium.edu.my

Received: February 7, 2024
Accepted: May 7, 2024
Published: July 31, 2024

DOI: https://doi.org/10.22452/mjs.vol43sp1.7
Malaysian Journal of Science 43 (Special Issue 1): 38-43 (July 2024)

eco-friendly activation aligns with the principles of sustainable development, fostering a circular economy approach while contributing towards the mitigation of climate change.

The objective of this study is to explore the potential of *MO* seed husk as a raw material for activated carbon synthesis, investigating its carbonization and activation characteristics with a Na_2CO_3. The results of this study will contribute to the ongoing efforts to develop environmentally friendly carbon capture technologies, incorporating sustainable raw materials into the production process. By utilizing *MO* seed husk, not only biomass waste can be reduced but also the sustainable utilization and transformation of biomass waste to wealth is promoted. This research has the potential to provide valuable insights into the feasibility of utilizing *MO* seed husk to produce activated carbon.

2. Method

Sun dried *MO* seeds were separated from their husks as shown in Figure 1. Next, the seed husk was grinded to powder form using a regular grinder. Following the approach of (Nedjai et al., 2021; Santos et al., 2020), *MO* seed powder was converted to activated carbon by chemical activation and thermal activation at 500 °C with a nitrogen flow of 0.2 L per minute in a lab scale furnace reactor. The pyrolysis time was 60 minutes (after the reactor reached the pyrolysis temperature) with a constant heating rate of 10 °C per minute. The reactor was heated with a custom heating mantle, and the temperature was checked with a type K thermocouple located inside the reactor. Before the pyrolysis process, chemical activation was performed on the ground *MO* seed shell powder (*MOSSP*), using KOH and Na_2CO_3 as activating agents with 1:1 impregnation ratio. The resulting chemically activated products are shown in Figure 2. The obtained carbon was dried in an oven at 105°C overnight. The mixture was then heated to the thermal activation temperature of 500˚C for 1 hour. The activated carbon produced after thermal activation is presented in Figure 3. After cooling, the resulting products underwent a thorough rinsing process using a 0.1 M HCl solution and warm distilled water until the pH reached 7.0. This rinsing procedure was employed to eliminate any residual activating agents and other inorganic substances that may have formed during the process. During the washing phase, the activated carbon was separated using Whatman filter paper. Subsequently, the obtained carbon was subjected to drying at 105°C until it achieved complete dryness, after which it was securely stored in tightly sealed centrifuge bottles for subsequent analysis. They

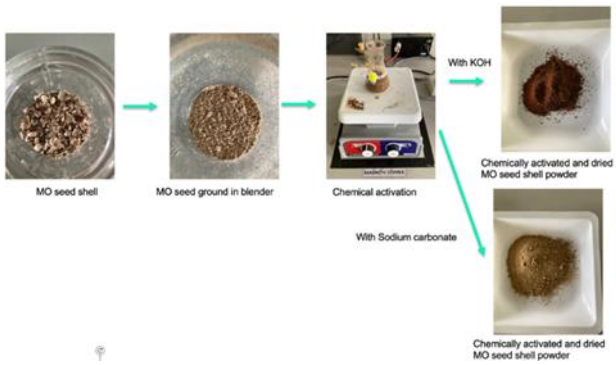

Figure 2. Summary of chemical activation process.

were analyzed for Brunauer-Emmett-Teller (BET), Fourier-Transform Infrared Spectroscopy (FTIR), X-ray Diffraction (XRD) and Scanning Electron Microscope (SEM) analyses.

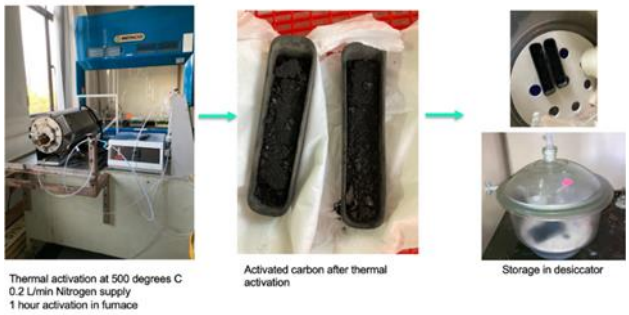

Figure 3. Thermal activation in furnace.

3. Results and discussion

This section discusses the resulting activated carbon properties in terms of SEM, FTIR, XRD and BET analyses.

3.1 SEM Analysis

The *MO* seed shell powder (*MOSSP*) was viewed under SEM, as shown in Figure 4 at x2000 magnification. Although most surfaces showed flat sheet type surfaces, some porous surfaces were observed as well. Having few porous structures before any chemical or thermal activation suggests potential inherent adsorptive ability of the seed husk powder. The SEM image depicts the morphology of the *MOSSP* in its natural form without any activation. Similar observation was made by Khalfaoui et al. (2022).

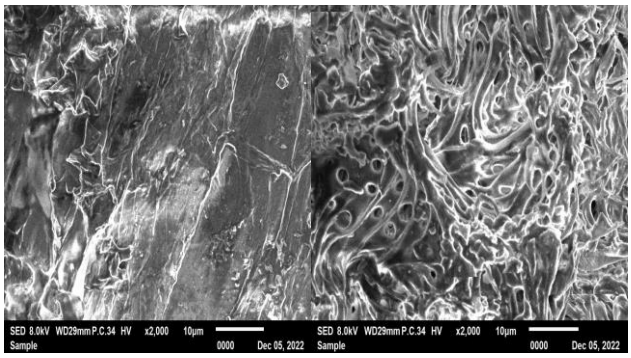

Figure 4. SEM images of raw *MO* seed shell powder at magnification x2000.

However, after chemical and thermal activation, more distinct porous structures were observed for both KOH and Na_2CO_3 based activation, as seen in Figures 5 and 6. *MOSSP* activated with Na_2CO_3 showed a pattern of mesopores inside circular fibrous structures (lignin), more prominently observed in x2000 magnification. This structure can potentially provide a good surface area for CO_2 adsorption, through the pores in the network of circular structures. By modifying the precursor surface, Nguyen et al. (2016) was able to produce mesoporous carbon with high CO_2 uptake with the largest mesoporous areas of the adsorbent.

DOI: https://doi.org/10.22452/mjs.vol43sp1.7
Malaysian Journal of Science 43 (Special Issue 1): 38-43 (July 2024)

With KOH activation, no fibrous structures were noted in the activated carbon, which is an indicator that KOH activation is strong enough to create smaller pores with higher density, while disintegrating all lignin from the *MOSSP*. The mild activating intensity of Na_2CO_3 resulted in the incomplete disintegration of the fibrous structures and hence, were still visible after activation at x1000 magnification (shown in Figure 5). The pores were further zoomed in with x2000 magnification in Figure 6. Notably, KOH activation produced smaller porous structures compared to Na_2CO_3 activation. KOH was able to produce smaller mesopores with higher BET surface area and pore volume in *MOSSP* compared to Na_2CO_3. The difference in mesopore development between KOH and Na_2CO_3 as activating agents for producing activated carbon can be attributed to their distinct activation mechanisms and chemical properties. KOH, being a strong activating agent, tends to promote more extensive and aggressive gasification and pore formation during activation (Sevilla et al., 2021). Its high reactivity leads to the creation of a larger number of mesopores within the activated carbon structure. In contrast, Na_2CO_3, while still effective, exhibits a more moderate activation strength, resulting in the formation of fewer but larger mesopores.

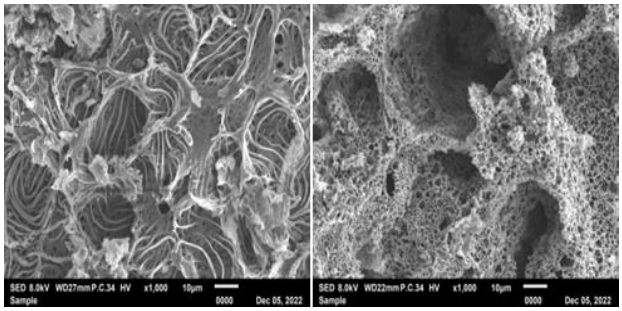

Figure 5. SEM image of *MO* seed shell synthesized with Na_2CO_3 (left) and KOH (right) activation at x1000 magnification.

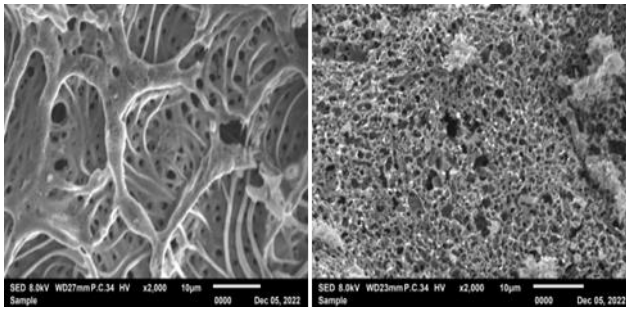

Figure 6. SEM image of *MO* seed shell synthesized with Na_2CO_3 (left) and KOH (right) activation at x2000 magnification.

3.2 XRD Analysis

X-ray diffraction (XRD) is vital for characterizing the prepared activated carbons, to identify their crystalline phases, detect impurities, and indirectly provide insights into pore structure that influences its adsorption capacity. It can spot defects in the material, quantify crystalline phases, reveal structural parameters, and guide process optimization and material development for various applications. Figure 7 depicts the X-ray diffractogram of *MOSSP* before (green) and after activation with KOH (red) and Na_2CO_3 (blue) activation. The broad peak (2θ) at 23° depicts the amorphous structure of the *MOSSP* and produced activated carbon (Prakash et al., 2020), which slightly shifted to 25° after conversion to activated carbon using both KOH and Na_2CO_3 activating agents. The peak shift observed in the XRD pattern of *MOSSP* after chemical and thermal activation are reflective of the changes occurring in the material's structure and composition. These changes are responsible for the development of a porous and highly adsorptive activated carbon material, making it suitable for various applications such as water treatment and CO_2 adsorption. Besides peak shift, there was an elevation of peak intensities after activated carbon production. Activation created a vast network of micro and mesopores within the activated carbon material. These pores provide additional scattering centres for X-rays, contributing to the increased intensity of the XRD peaks. The abundance of pores enhanced the diffraction efficiency of the activated carbon sample. However, a sharp peak at 27° for KOH activated carbon and 68.5° for Na_2CO_3 denotes the presence of possible impurities in the final activated carbon.

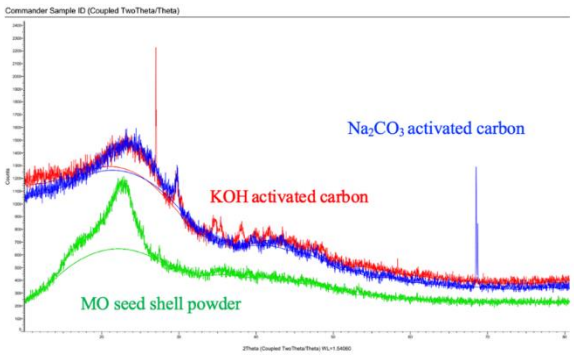

Figure 7. XRD graphs of *MOSSP* (green), *MO* activated carbon with KOH (red) and Na_2CO_3 (blue).

The sharp peaks in the XRD diffractogram of activated carbon can happen due to the presence of well-ordered crystalline regions within the material. During the activation process, certain conditions or precursor materials may lead to the development of these crystalline carbon regions. This occurs through processes like graphitization, where carbon atoms are arranged in repeating graphene layers, forming small crystallites (Zhang et al., 2022). Additionally, the presence of impurities or inorganic materials introduced during the activation process can also contribute to the appearance of sharp diffraction peaks. Overall, the sharp peaks were indicative of the structural complexity of the activated carbon, with crystalline regions providing additional adsorption sites and impurities potentially influencing its adsorption behaviour. Understanding the reasons for the sharp peaks helps in characterizing and optimizing activated carbon for various applications.

3.3 FTIR Analysis

FTIR analysis was conducted to characterize the prepared activated carbons by detecting surface functional groups and chemical bonds, evaluating composition and purity, and investigating the impact of surface modifications. Figure 8 shows the FTIR spectra of *MOSSP* alongside of KOH and Na_2CO_3-AC activated carbons. Overall, the *MOSSP* spectrum exhibited more

DOI: https://doi.org/10.22452/mjs.vol43sp1.7
Malaysian Journal of Science 43 (Special Issue 1): 38-43 (July 2024)

absorption peaks compared to the KOH-AC and Na_2CO_3-AC spectra. Upon activation, several peaks present in the *MOSSP* disappeared in the activated carbon spectra, indicating structural changes resulting from the activation process. This was due to the elimination of heat-sensitive functional groups at high temperatures and volatiles (Nedjai et al., 2021).

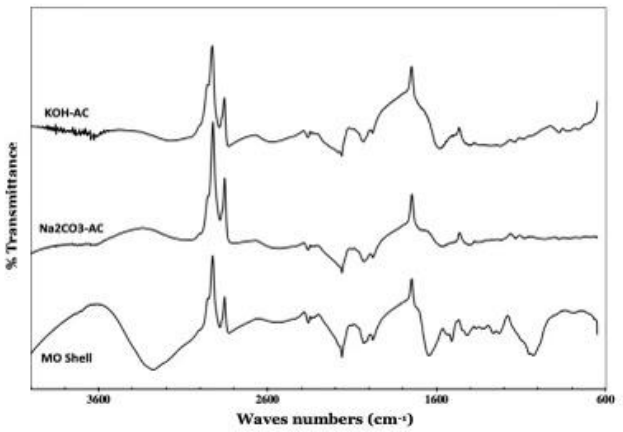

Figure 8. Fourier Transform Infra-Red Spectra for *MO* shell and KOH and Na_2CO_3 activated carbons.

For the *MOSSP* (not activated), the broad band at 3278 cm^{-1} is a characteristic of a stretching vibration of hydrogen-bonded (O-H) hydroxyl groups. The peaks appearing at 2881 and 2828 cm^{-1} are described to (C–H) symmetric stretching and ($–CH_2$) alkyl groups. The bands observed at 2160 cm^{-1} and 2029 cm^{-1} were due to the presence of (C≡N) stretching (Prahas et al., 2008; Vunain & Biswick, 2019). Another peak noted at 2358 cm^{-1} is related to the (C≡N) stretching vibration. The band at around 1644 cm^{-1} is the (C=O) stretching vibration due to the bonds of esters and phenols (Jawad & Abdulhameed, 2020), which disappeared in KOH-AC and Na_2CO_3-AC. The peak observed at 1509 cm^{-1} corresponds to the secondary amine group. Other bands, recorded at 1422 cm^{-1} and 1229 cm^{-1} are attributed to CH_3 asymmetric bending and C-O stretching, respectively. A peak situated at around 1027 cm^{-1} depicted the characteristics of anhydrides (C–O), which also disappeared completely after the chemical activation.

For Na_2CO_3-AC, the FTIR spectroscopic analysis indicated the presence of different peaks at 3055 cm^{-1}, 2881 cm^{-1}, 2529 cm^{-1}, 1556 cm^{-1}, 1408 cm^{-1} which were the characteristics of O–H (hydroxyls), C–H (alkyls), C≡C (alkyne), C–O–C (ester, ether and phenol) and CH_3 asymmetric bending, respectively. On the other hand, the FTIR spectrum of KOH-AC depicted broad weak peaks around 3897–3564 cm^{-1} and other peaks around 3175 cm^{-1}, 2885 cm^{-1}, 2574 cm^{-1}, 1574 cm^{-1}, 1225 cm^{-1}, and 847 cm^{-1}. These are the characteristics of O–H (hydroxyls), C–H (alkyls), C≡C (alkyne), C–O–C (ester, ether and phenol), C-O stretching, and C-H bending, respectively. The main functional groups in prepared activated carbons were, therefore, hydroxyl groups, carbonyl groups, and carboxyl groups, which indicated that the functional groups have been successfully stepped onto the surface of the activated carbons and contain binding sites of various natures.

3.4 BET Analysis

BET analysis was carried out on the prepared activated carbons to quantify their surface area and pore structure, to provide insights into the activated carbon's adsorption capabilities. Table 1 presents the results of the BET analysis for the three samples: KOH-AC, Na_2CO_3-AC, and *MOSSP* (no activation). It is evident that pore size plays a significant role in determining the CO_2 capture ability of Na_2CO_3-AC. While KOH-AC exhibited a smaller average pore diameter (5.8482 nm) and a higher BET surface area, Na_2CO_3-AC demonstrated larger average pore diameter (14.8646 nm). This difference in pore size indicated that Na_2CO_3-AC was characterized by larger mesopores and macropores, which are advantageous for capturing CO_2 molecules. These larger pores provide sufficient space and accessibility for CO_2 adsorption, enabling Na_2CO_3-AC to effectively capture and store CO_2. Although Na_2CO_3-AC has a lower BET surface area (18.4659 m^2/g) compared to KOH-AC (235.6034 m^2/g), its ability to accommodate CO_2 within its larger pores can potentially compensate for the surface area difference. Hence, the pore size distribution of Na_2CO_3-AC may contribute to its CO_2 capture ability, showcasing the importance of pore structure in determining the performance of green activated carbon materials.

Table 1. Summary of BET analysis results.

Sample	S_{BET}[a]	D_{Pore}[b]	V_t[c]
KOH-AC	235.6034 m^2/g	5.8482 nm	0.163380 cm^3/g
Na_2CO_3-AC	18.4659 m^2/g	14.8646 nm	0.041413 cm^3/g
MOSSP	0.9332 m^2/g	23.9764 nm	0.001688 cm^3/g

[a] BET surface Area
[b] Adsorption average pore diameter
[c] Single point adsorption total pore volume of pores

DOI: https://doi.org/10.22452/mjs.vol43sp1.7
Malaysian Journal of Science 43 (Special Issue 1): 38-43 (July 2024)

Mesopores, with pore sizes ranging from 2 to 50 nm, contribute to the effectiveness of CO_2 capture in activated carbons. While micropores play a dominant role in providing high surface area and strong interaction with CO_2 molecules, mesopores offer additional advantages. Their presence facilitates improved mass transfer and faster diffusion of CO_2 within the material. By providing larger pathways, mesopores can enhance the accessibility of CO_2 to the adsorption sites, leading to potentially more efficient adsorption. The reduced diffusion resistance within mesoporous structures enables a higher flow rate of CO_2, resulting in enhanced kinetics of the capture process (Azmi & Aziz, 2019).

4. Conclusion

In the context of CO_2 capture, it is important to note that pore size alone is not the sole determinant of the CO_2 capture ability of Na_2CO_3-AC. While pore size can influence the accessibility and diffusion of CO_2 molecules within the material, other factors such as surface chemistry, surface area, and pore volume also play crucial roles in determining the CO_2 adsorption capacity. Therefore, it is necessary to consider a comprehensive analysis of all these parameters to assess the CO_2 capture ability of Na_2CO_3-AC accurately. The choice between these agents depends on the desired pore structure and specific application requirements, with KOH offering greater mesopore development when it is needed for applications like gas adsorption and catalysis. Additionally, mesopores can be modified or coated to increase surface coverage and affinity for CO_2 adsorption.

Although, KOH based activated carbon in this study seemed to be a more favorable adsorbent material for CO_2 capture, employing Na_2CO_3 to produce the activated carbon from biomass waste such as *MO* seed husk, provided an insight on a greener adsorbent production strategy, that can be further explored.

5. Acknowledgement

The authors express gratitude to International Islamic University Malaysia, Faculty of Engineering, for the financial support under Tuition Fee Waiver (TFW) 2021 scheme. The authors also thank the Ministry of Education (MOE) Malaysia for granting a Fundamental Research Grant Scheme (FRGS), project no. FRGS/1/2019/TK02/UIAM/01/1 to support this work.

6. References

Abuelnoor N., AlHajaj, A., Khaleel M., Vega L. F. & Abu-Zahra M R M. (2021). Activated carbons from biomass-based sources for CO_2 capture applications. Chemosphere, 282(March), 131111, https://doi.org/10.1016/j.chemosphere.2021.131111.

Azmi A. A. & Aziz M. A. A. (2019). Mesoporous adsorbent for CO2 capture application under mild condition: A review. Journal of Environmental Chemical Engineering, 7(2), 103022, https://doi.org/10.1016/j.jece.2019.103022.

González-García P. (2018). Activated carbon from lignocellulosics precursors: A review of the synthesis methods, characterization techniques and applications. Renewable and Sustainable Energy Reviews, 82(August 2017), 1393–1414, https://doi.org/10.1016/j.rser.2017.04.117.

Jawad A. H. & Abdulhameed A. S. (2020). Statistical modeling of methylene blue dye adsorption by high surface area mesoporous activated carbon from bamboo chip using KOH-assisted thermal activation. Energy, Ecology and Environment, 5(6), 456–469, https://doi.org/10.1007/s40974-020-00177-z.

Khalfaoui A., Mahfouf E., Derbal K., Boukhaloua S., Chahbouni B. & Bouchareb R. (2022). Uptake of Methyl Red dye from aqueous solution using activated carbons prepared from Moringa Oleifera shells. 4(September), https://doi.org/10.1016/j.clce.2022.100069.

Nedjai R., Alkhatib M. F. R., Alam M. Z. & Kabbashi N. A. (2021). Adsorption Of Methylene Blue Onto Activated Carbon Developed From Baobab Fruit Shell By Chemical Activation: Kinetic Equilibrium Studies. IIUM Engineering Journal, 22(2), 31–49, https://doi.org/10.31436/iiumej.v22i2.1682.

Nguyen T. H., Kim S., Yoon M. & Bae T. H. (2016). Hierarchical Zeolites with Amine-Functionalized Mesoporous Domains for Carbon Dioxide Capture. ChemSusChem, 9(5), 455–461, https://doi.org/10.1002/cssc.201600004.

Prakash M. O., Raghavendra G., Ojha S. & Panchal M. (2020). Characterization of porous activated carbon prepared from arhar stalks by single step chemical activation method. Materials Today: Proceedings, 39(xxxx), 1476–1481, https://doi.org/10.1016/j.matpr.2020.05.370.

Prahas D., Kartika Y., Indraswati N. & Ismadji S. (2008). Activated carbon from jackfruit peel waste by H3PO4 chemical activation: Pore structure and surface chemistry characterization. Chemical Engineering Journal, 140(1–3), 32–42, https://doi.org/10.1016/j.cej.2007.08.032.

Raji Y., Nadi A., Mechnou I., Saadouni M., Cherkaoui O. & Zyade S. (2023). High adsorption capacities of crystal violet dye by low-cost activated carbon prepared from Moroccan Moringa oleifera wastes: Characterization, adsorption and mechanism study. Diamond and Related Materials, 135(February), 109834, https://doi.org/10.1016/j.diamond.2023.109834.

Santos T. M., de Jesus F. A., da Silva G. F. & Pontes L. A. M. (2020). Synthesis of activated carbon from oleifera moringa for removal of oils and greases from the produced water. Environmental Nanotechnology, Monitoring and Management, 14(August), https://doi.org/10.1016/j.enmm.2020.100357.

Serafin J., Ouzzine M., Cruz O. F., Sreńscek-Nazzal J., Campello Gómez I., Azar F. Z., Rey Mafull C. A., Hotza D. & Rambo C. R. (2021). Conversion of fruit waste-derived biomass to highly microporous activated carbon for enhanced CO_2 capture. Waste Management, 136(October), 273–282, https://doi.org/10.1016/j.wasman.2021.10.025.

DOI: https://doi.org/10.22452/mjs.vol43sp1.7
Malaysian Journal of Science 43 (Special Issue 1): 38-43 (July 2024)

Sevilla M., Díez N. & Fuertes A. B. (2021). More Sustainable Chemical Activation Strategies for the Production of Porous Carbons. ChemSusChem, 14(1), 94–117, https://doi.org/10.1002/cssc.202001838.

Yamaguchi N. U., Cusioli L. F., Quesada H. B., Camargo Ferreira M. E., Fagundes-Klen M. R., Salcedo Vieira A. M., Gomes R. G., Vieira M. F. & Bergamasco R. (2021). A review of Moringa oleifera seeds in water treatment: Trends and future challenges. Process Safety and Environmental Protection, 147(September), 405–420, https://doi.org/10.1016/j.psep.2020.09.044.

Varma R. S. (2019). Biomass-Derived Renewable Carbonaceous Materials for Sustainable Chemical and Environmental Applications. ACS Sustainable Chemistry and Engineering, 7(7), 6458–6470, https://doi.org/10.1021/acssuschemeng.8b06550.

Vunain E. & Biswick T. (2019). Adsorptive removal of methylene blue from aqueous solution on activated carbon prepared from Malawian baobab fruit shell wastes: Equilibrium, kinetics and thermodynamic studies. Separation Science and Technology (Philadelphia), 54(1), 27–41, https://doi.org/10.1080/01496395.2018.1504794.

Zhang S., Zheng M., Tang Y., Zang R., Zhang X., Huang X., Chen Y., Yamauchi Y., Kaskel S. & Pang H. (2022). Understanding Synthesis–Structure–Performance Correlations of Nanoarchitectured Activated Carbons for Electrochemical Applications and Carbon Capture. Advanced Functional Materials, 32, https://doi.org/10.1002/adfm.202204714.

DOI: https://doi.org/10.22452/mjs.vol43sp1.7
Malaysian Journal of Science 43 (Special Issue 1): 38-43 (July 2024)